Relaxations in electron beams and adiabatic acceleration

A. V. Aleksandrov, N. S. Dikansky, N. Cl. Kot, V. I. Kudelainen, V. A. Lebedev, and P. V. Logachov
Institute of Nuclear Physics, Novosibirsk, Russia

R. Calabrese and V. Guidi
Dipartimento di Fisica dell'Università, I-44100 Ferrara, Italy

G. Ciullo and G. Lamanna
Laboratori Nazionali di Legnaro, I-35020 Legnaro, Italy

L. Tecchio
Dipartimento di Fisica Sperimentale dell'Università, Torino, Italy
(Received 4 May 1992)

In order to produce electron beams with the minimum possible energy spread we have investigated the possibility of replacing the usual thermocathodes with a photoemissive source such as GaAs. A comparison carried out between these two sources indicated the latter as the best device to obtain a very-low-energy spread. Beam relaxation after emission also leads to an increase in the energy spread. Therefore an experimental study on the nature of relaxations occurring in electron beams, yielded both by a thermocathode and by a photocathode, has been performed. More specifically, we investigated the possibility of reducing the transverse-longitudinal and the longitudinal-longitudinal relaxations. With this aim, the features of adiabatic acceleration, which damp the pure longitudinal relaxation, have been examined. The experience gained during the measurement cycle demonstrated that an adiabatic structure, accelerating electrons emitted by a GaAs photocathode, leads to the best performances.

PACS number(s): 41.85.−p, 29.25.Bx

INTRODUCTION

Several research areas require electron beams with a narrow-energy-distribution function ($\Delta E < 100$ meV) in order to increase measurement accuracy and to analyze effects which would be negligible in a broader distribution. Beam current is another important parameter. For instance, an ultracold-electron beam for electron cooling, designed to cool ion beams so efficiently as to cause their crystallization [1], requires about 1-mA current and a longitudinal energy spread lower than 100 meV [2]. These requirements cannot be met with conventional thermocathodes, since emission of a given current density is attained by adjusting the operating temperature (Richardson's law) and, in turn, the related energy spread is too large.

Photoemission from semiconductors seems to constitute an excellent electron source, from the standpoint of energy spread [3]. GaAs photoemission characteristics have been extensively studied over the past few years [4,5]. Narrow energy distributions have been measured only at very low current (~ 1 nA) so far. Recently the use of a single-mode Ti:Al_2O_3 laser, tuned to 800 nm, allowed us to generate an electron beam with a longitudinal energy spread at the cathode of $\Delta E_{\|0} = 85$ meV [full width at half maximum (FWHM)] and, at the same time, a 100 μA current [6].

The problem then arises from accelerating such a low-energy-spread beam up to the required energy for each specific application, without excessively increasing the energy spread itself. In fact, after being emitted, the electron charge is no longer shielded by lattice nuclei; this causes a strong increase in the energy spread unless this is controlled somehow. Two types of interaction may be distinguished in the beam: one along the acceleration axis and another in the transverse direction. It will be shown later how these two interactions have different dynamic behaviors, hence two different compensation schemes have to be provided. The transverse effect can be prevented by means of a strong axial magnetic field, while it is necessary to use a specially designed accelerating structure (allowing for adiabatic acceleration, as we shall discuss later) to cope with the problem arising in the longitudinal direction.

A previous preliminary study joining both the benefits of the low-energy-spread photoemission from GaAs and adiabatic acceleration allowed the observation of experimental evidence of an electron beam with a plasma parameter $\Gamma_{\|}$ [7] larger than 1 [8], which is associated with a beam average potential energy larger than its longitudinal thermal energy. Computer simulations [9] predict a strong coupling in the electron motion for this system, so that for values of $\Gamma_{\|} \approx 3$ a liquidlike behavior is expected. These simulations, valid for a general electron or ion beam, also anticipate that a solid phase could occur at $\Gamma_{\|} \cong 170$ (Wigner's crystal [10]). We aim at using an electron beam with $\Gamma_{\|} > 1$ to reduce ion-beam temperatures, (electron-cooling technique), since this should allow us to obtain even more ordered states for the ion beams themselves (it is $\Gamma_{\|i} = Z^2 \Gamma_{\|}$ for the ion-plasma parameter $\Gamma_{\|i}$,

where Z is the ion charge [11]).

The present paper aims at a deeper understanding of the relaxation mechanisms, providing a more thorough study of the adiabatic acceleration in order to achieve a physical knowledge of these phenomena and to test design criteria for accelerating structures. Showing that the beam energy spread achieved by photoemission is lower than in the thermoemissive case, we also point out the different features in relaxation phenomena that thermo- and photoemitted beams present.

RELAXATION THEORY OF ELECTRON BEAMS AND ADIABATIC ACCELERATION

When an electron beam is accelerated, kinematic contraction (cooling) occurs along the acceleration axis z [12,13], provided that there is no energy transfer from the transverse degrees of freedom (not cooled by acceleration) into the longitudinal ones. A strong axial magnetic field can prevent such a transfer. The nonrelativistic relationship between the acceleration energy W and the longitudinal energy spread in the beam rest frame $\Delta E_{\parallel}$ is

$$\Delta E_{\parallel}=\frac{\Delta E_{\parallel 0}^2}{4W} . \tag{1}$$

This formula would be valid if the intrabeam scattering between electrons could be regarded as negligible. Indeed, experimental evidences indicate the opposite; at $W=500$ eV, even for values of the beam electron density as low as $n=10^5$ cm^{-3}, the contribution of the intrabeam-scattering term exceeds the right-hand-side term of Eq. (1) and starts being dominating. Equation (1) must therefore be changed as follows:

$$\Delta E_{\parallel}=\frac{\Delta E_{\parallel 0}^2}{4W}+Ce^2n^{1/3} , \tag{2}$$

where e is the electron charge and C is a constant value (of the order of unity) related to the accelerating structure and the energy W [8].

Acceleration causes inhomogeneity in the electron density along the longitudinal z axis because of the different electron velocities $v(z)$ experienced by the electrons being accelerated, while the current density $j=nev$ remains a constant of the motion. Intrabeam scattering contributes to make the density homogeneous while, however, increasing the energy spread. According to Ref. [13], such a density relaxation is called the longitudinal-longitudinal one. The time taken by this relaxation to occur is assumed to be the usual plasma characteristic time $\tau=2\pi/\omega_0$ [8,14], where $\omega_0=(4\pi e^2n/m)^{1/2}$ is the plasma frequency and m is the electron mass. By using Eq. (1), formula (2) can be expressed in the laboratory system, this being the frame of reference in which measurements are performed. Thus, the energy spread in the laboratory system ΔW is

$$\Delta W=[(\Delta E_{\parallel 0})^2+4Ce^2n^{1/3}W]^{1/2} . \tag{3}$$

We have so far discussed the case where the transverse degrees of freedom do not contribute to $\Delta E_{\parallel}$. Indeed, intrabeam scattering causes a relevant energy transfer from the transverse to the longitudinal direction: this is called transverse-longitudinal relaxation[13] or Boersch effect.[15] This relaxation lasts until equilibrium between longitudinal and transverse energy spreads is reached. When no magnetic field is applied, and for $\Delta E_{\parallel}\ll\Delta E_{\perp}$, ($\Delta E_{\perp}$ being the transverse energy spread), the effect of this relaxation can be expressed by the increase rate of transverse energy spread along z [16,17]

$$\frac{d(\Delta E_{\parallel})}{dz}=K\frac{\pi e^3jL_c}{W}\left[\frac{m}{\Delta E_{\perp}}\right]^{1/2} , \tag{4}$$

where L_c is the Coulomb logarithm and K is a coefficient depending on the electron distribution function (of the order of unity). As illustrated in this paper, along with the presentation of the experimental results, this relaxation strongly affects the energy spread $\Delta E_{\parallel}$. In this case the longitudinal-longitudinal relaxation has a minor contribution to $\Delta E_{\parallel}$. A strong magnetic field B causes a substantial change in the kinetics of electron collisions, and consequently also in the relaxation time.

An experimental method to find the required field strength consists of considering that the average cyclotron radius ρ of the electrons, in their magnetized motion, is much smaller than the average distance among them,

$$\rho\ll d=(4\pi n/3)^{-1/3} . \tag{5}$$

If the longitudinal energy spread is sufficiently small, the electron collisions have adiabatic characteristics and the energy transfer from the transverse to the longitudinal motion is therefore suppressed. Thus, the additional condition required to damp the transverse-longitudinal relaxation is that ρ must be much smaller than the minimal probable distance among electrons, which can be evaluated as $e^2/\Delta E_{\parallel}$,

$$\rho\ll e^2/\Delta E_{\parallel} . \tag{6}$$

Relationships (5) and (6) should be taken into account when designing accelerating structures which require minimal energy spread in the longitudinal direction.

Unfortunately, no relationship corresponding to Eq. (4) and taking into account also the magnetic-field effect exists, although empirical formulas have been proposed, which, however, fit experimental results only within a limited range in the current density and with a poor accuracy. As is well known [16] and confirmed by our experimental results (described hereafter), a sufficiently strong magnetic field can prevent transverse-longitudinal relaxation, while no relevant effect on the longitudinal-longitudinal relaxation has been recorded. At present, the only way to damp the longitudinal-longitudinal relaxation seems to consist of using the so-called adiabatic acceleration, i.e., where the acceleration time is much longer than the characteristic plasma period τ. In other words, this acceleration is so slow that the equilibrium between the potential and the kinetic energies of the electrons is maintained at any time by plasma oscillations; this condition is not met when the usual fast acceleration occurs.

Adiabatic acceleration lowers the value of constant C

in Eq. (2) and, consequently, the longitudinal energy spread is also reduced. A test carried out with this type of acceleration [8] yielded $C=1.2$, while it was found $C=3.8$ with a usual fast regime, accelerating the beam to the same energy in the two cases ($W=900$ eV). The energy spread was so narrow that the recorded plasma parameter $\Gamma_{\parallel}$ was larger than the one over a relatively wide current density range (1.0–6.4 mA/cm^2). Adiabatic acceleration therefore allowed the experimental observation of an electron beam under the condition $\Gamma_{\parallel}>1$.

A quantitative evaluation of the adiabaticity condition is provided by the nondimensional parameter λ, which compares the cooling time $[-d(\Delta E_{\parallel}/dt)/\Delta E_{\parallel}]^{-1}$ to the plasma characteristic time $\tau=1/\omega_0$,

$$\lambda=-\frac{1}{\omega_0\Delta E_{\parallel}}\frac{d(\Delta E_{\parallel})}{dt} . \tag{7}$$

Thus, an accelerating structure is defined as adiabatic if $\lambda<1$. For instance, the standard Pierce optics system [19] has $\lambda=2^{3/2}$, i.e., nonadiabatic characteristics.

EXPERIMENTAL SETUP

Two electron sources were used to generating the electron beam. One was the usual BaO thermocathode; the second was a GaAs photocathode, activated in negative-electron-affinity (NEA) conditions [3] by means of a thin layer of cesium and oxygen deposited on the surface. Laser excitation was supplied by at 450-mW Ti:Al_2O_3, operating in the wavelength range of 780–850 nm. The emission capability of this source has been summarized in Ref. [20]. For an 800-nm wavelength, a 1.2% quantum yield was recorded, with a 48-h lifetime in a 5×10^{-11} Torr vacuum environment; the photocathode can then be renewed by repeating the cesium-oxygen treatment [4,20]. Both sources were installed in the accelerating structure (Fig. 1), the main parameters of which are summarized in Table I. The experimental setup is fully described elsewhere [21]. The whole structure was immersed in an axial magnetic field ranging between 0.6 and 4.0 kG.

In order to draw the maximum possible current, while overcoming any space-charge effects, a Pierce optics has been designed between cathode and anode, whereas a small (2-mm) gap between these was selected to ensure a high extraction value. After a first fast acceleration step,

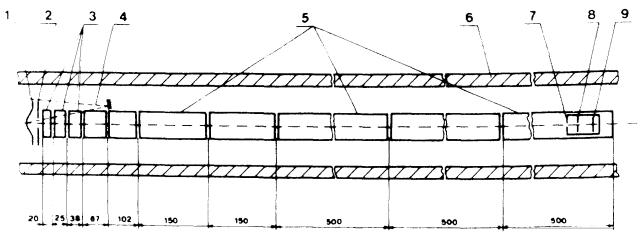

FIG. 1. Sketch of the experimental installation: 1, cathode; 2, anode; 3, adiabatic structure tubes; 4, laser beam; 5, drift space tubes; 6, solenoid; 7, diaphragm; 8, retarding electrode; 9, collector. Dimensions are expressed in mm.

TABLE I. Main parameters of the experimental device.

Pressure	4×10^{-11} mbar
Electron energy	0–900 eV
Electron beam current	0.001–10 mA
Electron beam radius	0.25–1 mm
Magnetic field intensity	0.64–4 kG
Solenoid length	2.88 m
Accelerating structure length	0.25 m
Length of the drift section	1.8 m

the electron beam enters an adiabatic acceleration area consisting of five 16-mm diam pipes. In order to have a constant value of the adiabatic parameter λ, the potential $V(z)$ was distributed over the pipe electrodes according to the relationship $V(z)=K\{(z-z_0)+[V(z_0)/K]^{3/4}\}^{4/3}$, where z_0 and $V(z_0)$ are the position and potential for the first adiabatic electrode, respectively. The constant $K\cong11$ V/cm$^{4/3}$ is determined so as to meet the $\lambda<1$ adiabaticity condition, which is required to damp the longitudinal-longitudinal relaxation during acceleration. In the case of fast acceleration, the pipes are connected to ground potential so that acceleration occurs only from the cathode to the anode and to the first adiabatic electrode. Electrons move along the solenoid axis to the energy analyzer, serving also as a collector. The latter can be moved between 0.3 and 1.8 m away from the cathode surface. The measurement method is based on the analysis of the energy spread in a thin electron beam, bled off the main stream through a small 50-μm-diam hole. The electron beam is decelerated adjusting the retarding electrode potential (see Fig. 1) relative to the cathode one; at the same time the current flowing in the collector is measured. This receives only electrons with an energy greater than the potential energy $E=eV_d$, V_d being the retarding potential. This allows us to measure $\int_0^E(dn/dE')dE'$, dn/dE' being the energy distribution function of the beam. We then fit the experimental data, through the least-squares method, with the integral of a Gaussian distribution. The energy spread is then the FWHM of the energy-distribution function. The energy resolution of the experimental device turns out to be linear versus the beam energy and is about 8 meV at $W=900$ eV [21].

MEASUREMENT RESULTS

The first step consisted of analyzing the time taken by an electron beam to develop its longitudinal-longitudinal relaxation. The beam, emitted by the thermocathode, was accelerated at low energy (50 eV) until electrons entered the first gap between the pipes (see Fig. 1), then accelerated to full energy (800 eV) and collected by the energy analyzer. Figure 2 illustrates the longitudinal energy spread $\Delta E_{\parallel}$ versus the time of flight; both values are normalized with respect to the average electrostatic energy $e^2n^{1/3}$ and to the plasma oscillation period τ, respectively. It is clear that in a certain time, estimated to be about 0.4τ ($\sim10^{-8}$ s), the longitudinal energy spread $\Delta E_{\parallel}$ reaches its maximum value; after this, one or two further plasma oscillations establish the equilibrium

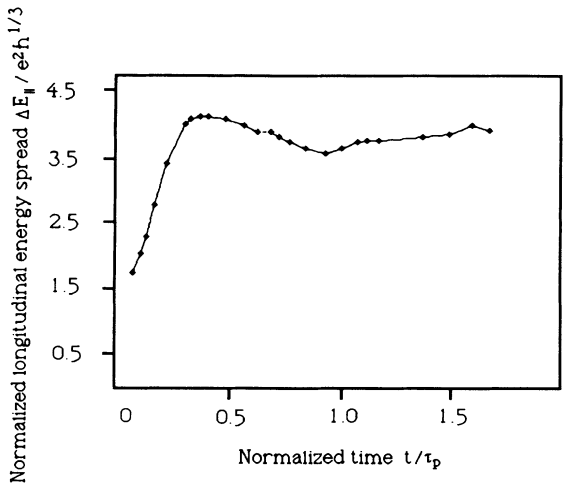

FIG. 2. Experimental trend of normalized longitudinal electron energy spread $\Delta E_{\parallel}$ vs normalized time after a fast acceleration for the oxide thermocathode; $I=300$ μA, $W=800$ eV, $n=3.73\times10^7$ cm^{-3}, $B=3$ kG.

value. These measurements confirm that the criterion of taking the plasma oscillation time as the longitudinal-longitudinal relaxation time is legitimate. This is not obvious since τ is the relaxation time for quasineutral plasmas where a positive background provides charge compensation; indeed an electron beam is charged and the Coulomb interaction is offset by the focusing force of the magnetic field.

Figure 3 illustrates the longitudinal energy spread ΔW of the photoemitted electron beam as a function of current density for three different energies W [9 eV (a), 100 eV (b), 400 eV (c)], with a constant 3-kG magnetic field. From Fig. 3 one can see that for $j\rightarrow0$ it is $\Delta W\rightarrow\Delta E_{\parallel0}=85$ meV as reported in Ref. [6]. It is also clear that the energy spread ΔW in the laboratory system

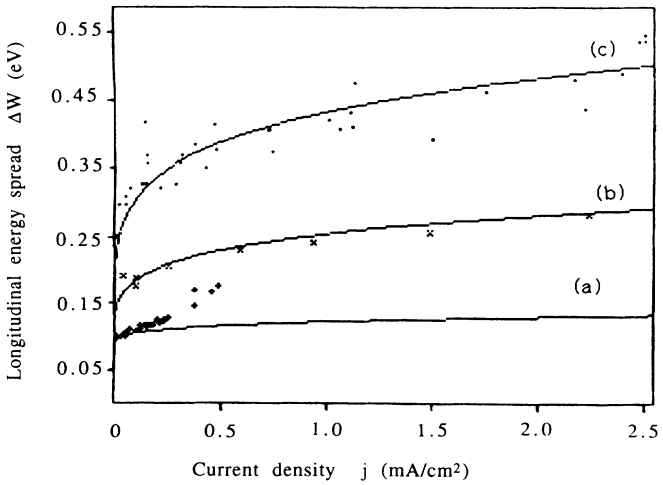

FIG. 3. Longitudinal energy spread ΔW for the photocathode vs current density for different beam energies: $W=9$ eV (+), $W=100$ eV (×), $W=400$ eV (●). The magnetic field was set at 3 kG. Curves (a), (b), and (c) are built by using Eq. (3) with $C=3.8$, $\Delta E_{\parallel0}=85$ meV.

depends on W. The two plots at higher energy are examples of pure longitudinal-longitudinal relaxation and fit Eq. (3) rather well, with $C=3.8$. This is not the case for $W=9$ eV, indicating that the time of flight is comparable with the transverse-longitudinal relaxation time; this affects the relaxation dynamics by increasing the longitudinal energy spread.

Experiments performed at the Antiproton Storage Ring of Novosibirsk (known as NAP-M) [16] and the "solenoid model" [22] provided only partial information on the behavior of beam relaxation along the z axis. The movable energy analyzer allows accurate measurements

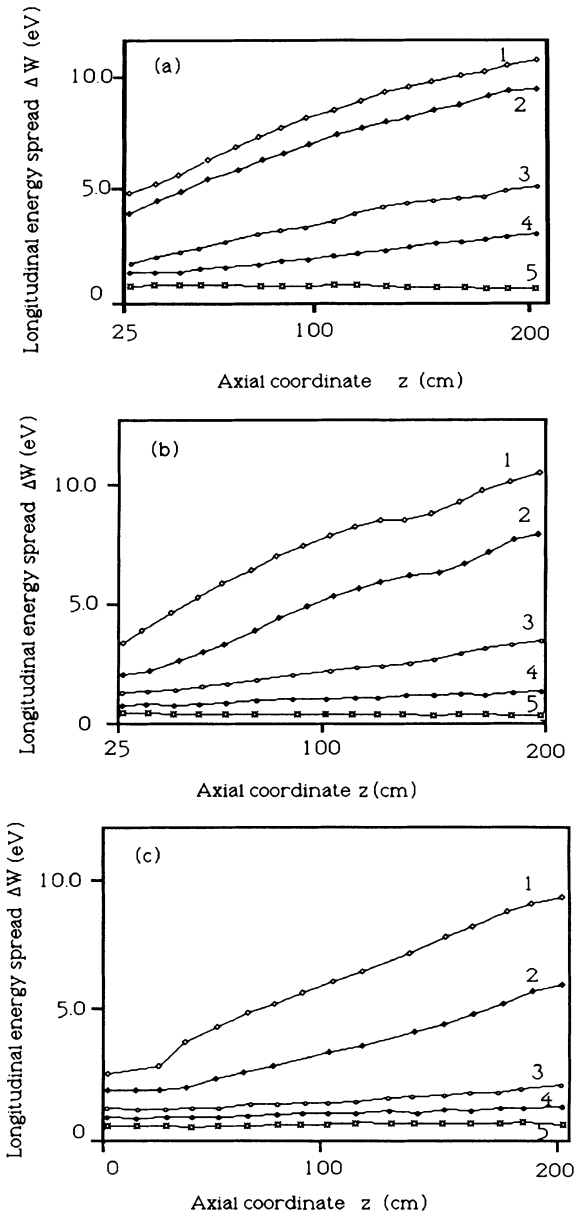

FIG. 4. Longitudinal energy spread ΔW for the oxide thermocathode vs the longitudinal z coordinate at various beam currents: 1, 9000 μA; 2, 6400 μA; 3, 3200 μA; 4, 1600 μA; 5, 100 μA; and for different values of the magnetic field: (a) $B=1$ kG, (b) $B=2$ kG, (c) $B=3$ kG. In all cases is $W=470$ eV.

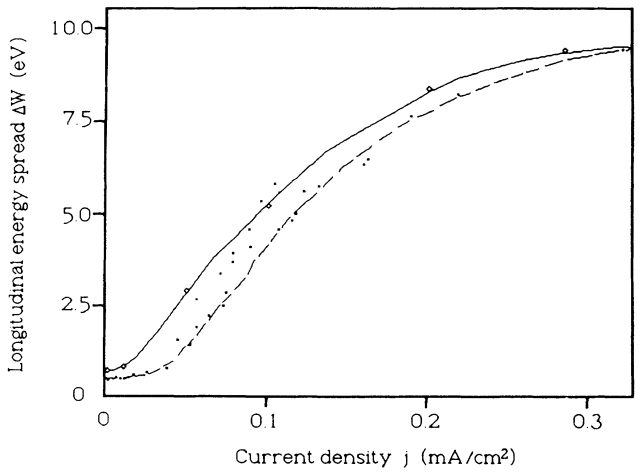

FIG. 5. Longitudinal energy spread ΔW vs beam current density for a thermocathode (◇) and photocathode (●) at 1 kG magnetic field for fast acceleration.

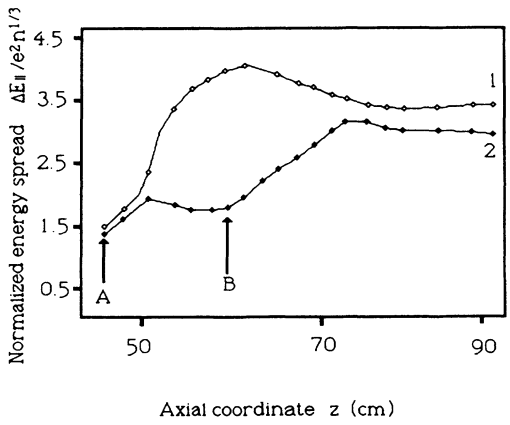

FIG. 6. Relationship of the normalized longitudinal energy spread $\Delta E_{\parallel}/e^2 n^{1/3}$ vs the z coordinate for fast acceleration (1) and a two-stage acceleration with intermediate drift space (2); $I=100\ \mu$A, $W=800$ eV, $B=3$ kG for the oxide thermocathode. A is the position of the first acceleration gap, B is the second one.

along this direction. The relationship between the longitudinal energy spread and z is illustrated in Figs. 4(a)–4(c) for several values of beam current and magnetic field, in the ranges 100–9000 μA and 1–3 kG, respectively. In this case the beam is generated by a thermocathode, with $W=470$ eV. It is evident that the stronger the magnetic field, the higher the damping of the transverse-longitudinal relaxation. In fact, a 1-kG axial field maintains the ΔW practically unchanged only for a 100-μA beam current, while in a 3-kG field the longitudinal energy spread does not change even for current values as high as 3200 μA.

With the energy analyzer located at its far end position the beam energy spread was measured as a function of the current density for the thermocathode and photocathode, at $B=1$ kG (Fig. 5). Comparing ΔW for $j\rightarrow 0$ in Fig. 5, namely when any contribution due to relaxations is negligible, the energy spread recorded with the photocathode is lower than with the thermocathode ($\Delta E_{\parallel 0\ \text{phot}} < E_{\parallel 0\ \text{ther}}$). When the transverse-longitudinal relaxation starts being relevant, the increase of ΔW is very fast (up to some eV) and no relevant difference appears between the photocathode and the thermocathode. Similarly the flat portion of the curve for the photocathode is caused by a lower transverse energy spread at the cathode $\Delta E_{\perp 0}$ (laboratory frame).

It is now necessary to investigate more closely the operating principle of adiabatic acceleration. Moving the energy analyzer along the z axis, the longitudinal energy spread ΔW for the thermocathode was measured at different locations; these measurements, expressed in dimensionless units, are illustrated in Fig. 6. Curve 1 records the values for a fast acceleration up to $W=800$ eV, taking place at the position A. The same final energy W was obtained in a two-stage acceleration at A and B; the intermediate energy supplied at A was $W=250$ eV. A comparison of these curves indicates that when the accelerating regime is such that it allows beam relaxation during the acceleration phase, this results in a smaller final longitudinal energy spread. This is, of course, a rough way to accelerate, but it clearly indicates the effect of adiabatic acceleration on the longitudinal relaxation.

Figure 7 shows the behavior of the longitudinal energy spread $\Delta E_{\parallel}$ for the thermocathode along z, after a fast and an adiabatic acceleration, respectively. The difference in the initial energy spread ($z=35$ cm) is related to the damping of longitudinal-longitudinal relaxation induced by adiabatic acceleration. The growth in the energy spread along the z axis is caused by transverse-longitudinal relaxation.

Figure 5 showed the minimal energy spread $\Delta E_{\parallel}$ obtained by using a photocathode and a fast acceleration. By virtue of the larger damping of the longitudinal-longitudinal relaxation provided by adiabatic acceleration, one could try to assemble this accelerating structure together with the NEA photocathode. At the same time the effect of the transverse-longitudinal relaxation must

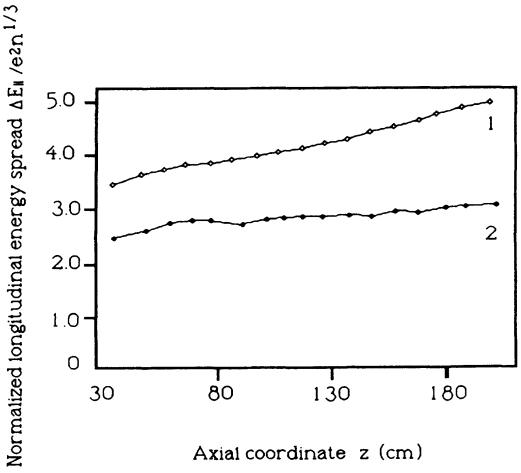

FIG. 7. Normalized longitudinal energy spread $\Delta E_{\parallel}/e^2 n^{1/3}$ for the thermocathode vs the axial z coordinate after fast (1) and adiabatic (2) acceleration; $W=470$ eV, $I=200\ \mu$A.

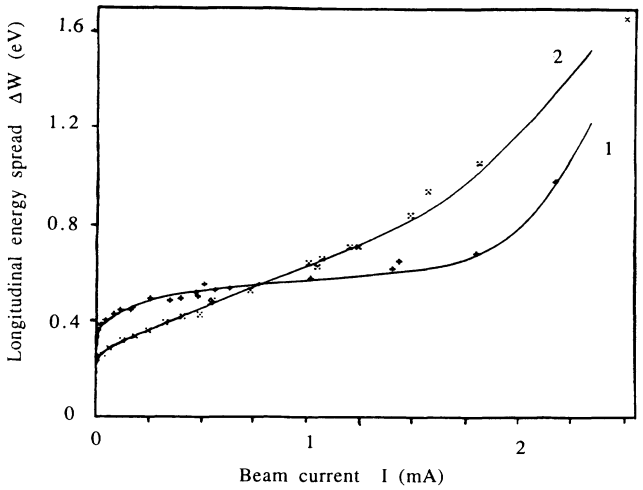

FIG. 8. Longitudinal energy spread ΔW for the photocathode vs collector current I at $W=900$ eV and $B=4$ kG: 1, fast acceleration; 2, adiabatic acceleration.

be taken into account; curve (a) of Fig. 3 already indicated this effect. The energy transfer by the Boersch effect is a serious problem because it might limit applicative possibilities of adiabatic acceleration. In fact, this slow longer-time-requiring acceleration permits a higher energy transfer from the transverse degrees of freedom. Figure 8 illustrates this effect; the longitudinal energy spread ΔW, at small beam current, is lower for the adiabatic case as we observed so far. Yet, the opposite behavior occurs when the current is increased since the Boersch effect is significant mostly for the adiabatic regime. Hence adiabatic acceleration seems to be disadvantageous for high currents (greater than 1 mA, such as in Fig. 8), unless the magnetic field is adequately strengthened to counteract the transverse-longitudinal relaxation. Unfortunately the required higher values of the magnetic field exceed the availability range of our device ($B_{\max}=4$ kG).

CONCLUSIONS

The present paper has examined the features of a GaAs crystal activated in a NEA condition as a photoemissive source. Comparison with a usual thermocathode shows that both the longitudinal energy spread at the source and the transverse one are lower in the photocathode case. Experimental results also indicate that this source works better at any regime, both varying the current density and changing the magnetic field.

A thorough study on the best fashion of electron acceleration just after emission has been performed. The nature of the two kinds of relaxations occurring in an electron beam during acceleration has been the object of investigation. In these measurements the movable energy analyzer played a fundamental role. We counteracted the transverse-longitudinal relaxation by imposing a sufficiently strong magnetic field, while in order to cope with the longitudinal-longitudinal one a specifically designed acceleration scheme is requested: adiabatic acceleration. We showed that when all the requirements for this slower acceleration are fulfilled (magnetic-field intensity, acceleration time), energy spreads lower than in a usual accelerating structure are obtained.

Finally, we remark that a structure, which adiabatically accelerates electrons produced by a GaAs photocathode, leads to minimal energy spreads. This device would be of great help for electron-cooling experiments since it should enhance the cooling efficiency, thus opening the possibility of observing ion-beam crystallization.

ACKNOWLEDGMENTS

This work has been partially supported by Istituto Nazionale di Fisica Nucleare and by Ministero della Università e della Ricerca Scientifica e Tecnologica of Italy. The authors acknowledge G. Bisoffi for the critical reading of the manuscript.

[1] For a complete view on crystalline beams see Proceedings of the Workshop on Crystalline Ion Beams, Wertheim, 1988, edited by R. W. Hesse, I. Hofmann, and D. Liesen, GSI Report No. 89-10, Darmstadt, Germany, 1989.
[2] R. Calabrese and L. Tecchio, Nuovo Cimento A **104**, 1127 (1991).
[3] R. L. Bell, *Negative Electron Devices* (Clarendon, Oxford, 1973), pp. 33–42 and 63–65.
[4] H. J. Drouhin, C. Hermann, and G. Lampel, Phys. Rev. B **31**, 3859 (1985); **31**, 3872 (1985).
[5] U. Kolac *et al.*, Rev. Sci. Instrum. **59**, 1933 (1988).
[6] A. V. Aleksandrov *et al.*, Phys. Lett. A **163**, 77 (1992).
[7] S. Ishimaru, Rev. Mod. Phys. **54**, 1017 (1982).
[8] A. V. Aleksandrov *et al.*, Europhys. Lett. **18**, 151 (1992).
[9] J. P. Schiffer and O. Poulsen, Europhys. Lett. **1**, 55 (1986); A. Rahman and J. P. Schiffer, Phys. Rev. Lett. **57**, 1133 (1986).
[10] A. L. Fetter and J. D. Walecka, *Quantum Theory of Many-Particle Systems* (McGraw-Hill, New York, 1971), 21–31.
[11] J. P. Schiffer, Z. Phys. A **321**, 181 (1985).
[12] H. Poth, Phys. Rep. **196**, 135 (1990).
[13] N. S. Dikansky *et al.*, Internal Report No. 88-61, Novosibirsk, 1988.
[14] D. Habs *et al.*, Phys. Scr. **T22**, 269 (1988).
[15] H. Boersch, Z. Phys. **139**, 115 (1954).
[16] V. I. Kudelainen *et al.*, Zh. Eksp. Teor. Fiz. **83**, 1153 (1982) [Sov. Phys. JETP **56**, 1192 (1982).].
[17] A. V. Aleksandrov *et al.*, *Proceedings of the Workshop on Electron Cooling and New Cooling Techniques,* edited by R. Calabrese and L. Tecchio (World Scientific, Singapore, 1991), p. 279.
[18] N. S. Dikansky *et al.*, in *Proceedings of the XIII International Conference on High Energy Accelerators,* edited by A. N. Skrinsky (Nauka, Novosibirsk, 1987), p. 330.
[19] J. R. Pierce, *Theory and Design of Electron Beams* (Van Nostrand, New York, 1954).
[20] R. Calabrese *et al.*, Meas. Sci. Technol. **1**, 665 (1990); J. Phys. III **2**, 473 (1992).
[21] A. V. Aleksandrov *et al.* (unpublished).
[22] N. S. Dikansky *et al.*, in *Proceedings of the First European Particle Accelerators Conference,* edited by L. Tazzari (World Scientific, Rome, 1988), p. 529.